# Prediction of shear wave velocity based on a statistical rock-physics model and Bayesian theory

Bing Zhang [a,b], Shuanggen Jin [b,c,*], Cai Liu [d], Zhiqi Guo [d], Xiwu Liu [e]

[a] Key Laboratory of Meteorological Disaster, Ministry of Education (KLME)/ Joint International Research Laboratory of Climate and environment Change (ILCEC)/ Collaborative Innovation Center on Forecast and Evaluation of Meteorological Disasters (CIC-FEMD), Nanjing University of Information Science and Technology, Nanjing, 210044, China
[b] School of Remote Sensing and Geomatics Engineering, Nanjing University of Information Science and Technology, Nanjing, 210044, China
[c] Shanghai Astronomical Observatory, Chinese Academy of Sciences, Shanghai, 200030, China
[d] College of GeoExploration Science and Technology, Jilin University, Changchun, 130012, China
[e] SinoPEC Petroleum Exploration and Production Research Institute, Beijing, 100083, China

## A R T I C L E   I N F O

## A B S T R A C T

Shear wave velocity ($V_s$) is essential for amplitude-variation-with-offset (AVO) analysis and reservoir characterization. However, $V_s$ is unavailable in many well logs due to the cost or the absence of technology for old wells. A common method is to estimate $V_s$ from other measurements through their relationships, but has a large uncertainty. In this study, a statistical method is proposed to predict $V_s$ of wells. Firstly, a statistical rock-physics model is built for the relationship between logging curves and $V_s$, which is realized by initializing key petrophysical parameters of the Xu–White model by the distributions instead of constants. The distributions come from prior information, which is a knowledge or experience of research area. Secondly, the key petrophysical parameters are calculated in Bayesian inversion framework by comparing the modeled compression wave velocity ($V_p$) with real data. Then, $V_s$ is estimated based on these parameters and the rock-physics model. The real data test shows that our statistical method gets accurate $V_s$ prediction, whose mean square error is about 0.002. Besides, the correlation coefficient between estimation and real data is about 0.97. The result is better than common methods. Moreover, statistics of the prediction, such as a confidence interval, can be provided by the statistical method. The real velocities are in the 95% confidence interval of the estimation. The estimated values and statistics of well velocities will offer more valuable information for the following processes of reservoir characterization.

## 1. Introduction

Shear wave velocity ($V_s$) is important for pre-stack seismic property analysis. In addition, $V_s$ is also necessary for petrophysical parameters inversion in reservoir characterization. However, $V_s$ is not always available in old wells and even some new wells. Borehole condition, logging technology and cost are reasons of the absence of $V_s$. Therefore, estimation of $V_s$ for these wells is significant.

There are various approaches to estimate $V_s$ of wells from other measurements, including well-logging data and core test. The empirical-formula-based methods build simple and direct relationships between $V_s$ and well-logging data. Castagna et al. (1985) constructed linear relationships between $V_s$ and compression wave velocity ($V_p$). Han et al. (1986) improved relationship of velocities, porosity and clay content. And also new equations are provided for rock in different pressures. Castagna and Backus (1993) built the relationship

between $V_s$ and $V_p$ by the least-square polynomial fitting for experimental data. Yan et al. (2002) combined Han's equation and Xu–White model to get a new fitting equation, and effect of aspect ratios on velocities was considered. Dvorkin and Mavko (2014) proposed that different empirical-formula-based $V_s$ predictors will not necessarily affect seismic-based hydrocarbon indicators. The reason may be that these methods have less accuracy for large scale prospecting. Vernik et al. (2018) investigated a hybrid technique based on Greenberg–Castagna method to take kerogen into account, and the $V_s$ prediction is improved. Though the empirical relationships are simple, they are common choices. Because conventional logging data, such as $V_p$, porosity and clay content, are enough for these methods. In recent years, intelligent predictors based on machine learning and artificial neural networks are emerging (Rajabi et al., 2010; Ranjbar-Karami et al., 2014; Zhang et al., 2020). The intelligent predictors can get accurate

---

* Corresponding author.
*E-mail addresses:* sgjin@shao.ac.cn, sg.jin@yahoo.com (S. Jin).

$V_s$ estimation, whose mean square error (MSE) is usually lower than 0.02 (Rajabi et al., 2010) and the correlation coefficient can reach 0.98 (Zhang et al., 2020). But these approaches need real data of target parameters, such as $V_s$, to train the system, and therefore lack extrapolation beyond the range of training data (Asoodeh and Bagheripour, 2012). In general, empirical equations and intelligent systems build direct but simplified relationships between $V_s$ (or modulus) and other conventional well logs. These methods are data-based. Because the relationships are built by data operation using fitting or intelligent systems, and the physical mechanisms of rock are not considered. However, empirical predictors are less accurate, and intelligent predictors are complex and absence of extrapolation.

Rock-physics models describe effects of microstructure on the integral attributes of rock, and thus can build relationships between velocities or modulus and microstructure properties. Model-based predictors using rock-physics models have been common choices in recent years. Xu and White (1995, 1996) proposed a model which built the relationship between velocities and pores and clay content for shaly sandstone. Xu and Payne (2009) extended the Xu–White model to carbonate rock and divided pores into four types to account the effect of different pores. There are also some more complicated models, in which velocities or modulus are related to many components of rock. The self-consistent model (SCM) (Berryman, 1980) assumed rock is a mixture of components which are ellipsoid with different aspect ratios. Guo and Li (2015) estimated $V_s$ using SCM for the Barnett Shale with given property, aspect ratio, and volume fraction of each component of rock. Ruiz and Dvorkin (2010) proposed an improved $V_s$ predictor based on the differential effective medium (DEM) theory by using a constant aspect ratio, which is about 0.13. Bai et al. (2013) used variable aspect ratios in Xu–White model, instead of common fixed aspect ratios. The changeable aspect ratio makes $V_s$ prediction more accurate. Tan et al. (2015) proposed an $V_s$ predictor for gas-bearing shale, in which different models are compared to get modulus of dry matrix. The reason is that gas-bearing shale has more complex components than regular sandstone. Sohail and Hawkes (2020) evaluated empirical and rock physics models for $V_s$ estimation, and thought modified Xu–White model is the best option available at present. As a consequence, predictors based on rock-physics models may provide better $V_s$ prediction than the empirical predictors, but many petrophysical parameters are necessary in the methods, which demands more well-logging data and core data. To extend the application of model-based predictors, the demands on real data should be reduced.

In this study, we propose a statistical method for $V_s$ prediction. Firstly, a statistical rock-physics model is built by analyzing the key petrophysical parameters which affect velocities in Xu–White model and initializing them with distributions from prior information instead of constants. The Xu–White model is a common choice for $V_s$ prediction and can be used in traditional well logging. Secondly, the key petrophysical parameters are calculated by matching modeled and real $V_p$ based on the statistical rock-physics model and Bayesian inversion theory. Subsequently, these parameters are used to estimate $V_s$ of wells. Real data test is performed in three field wells to validate the statistical predictor. The statistical rock-physics model and prior information are combined by Bayesian theory to improve accuracy of velocities estimation, and meanwhile additional statistics of the result are conducted.

## 2. Theory and methodology

### 2.1. Data-based methods for S-wave velocity calculation

Rock is made up by minerals, pores and fluids. The empirical and intelligent methods are based on data to build relationships between different properties of rock. The data usually comes from well logs and experiments. A benefit of these methods is that target physical parameters are related to measurements directly. Empirical equations are usually built by fitting. Han et al. (1986) proposed equations for shaly sandstone in different pressure based on experiments. Velocities are linear related with porosity ($\phi$) and clay content ($C$) in the equations. In 40Mpa confining pressure,

$$V_p\,(\text{km/s}) = 5.59 - 6.39\phi - 2.18C \tag{1}$$

$$V_s\,(\text{km/s}) = 3.52 - 4.91\phi - 1.89C \tag{2}$$

Although the empirical methods are simple and widely used, their accuracy is low.

Intelligent methods use complex and advanced algorithms instead of simple fitting. Rajabi et al. (2010) gave an equation based on genetic algorithm:

$$V_s = \beta_1 \text{LLD}^{\beta_2} + \beta_3 \text{NPHI}^{\beta_4} + \beta_5 \text{RHOB}^{\beta_6} + \beta_7 \tag{3}$$

where LLD, NPHI and RHOB are well logs; $\beta_1$, $\beta_2$, $\beta_3$, $\beta_4$, $\beta_5$, $\beta_6$ and $\beta_7$ are parameters given by the algorithm. Recently, machine learning and neural network are widely used in geophysics (Zhang et al., 2018a; Hui et al., 2019; Jia et al., 2019). Some intelligent predictors based on these algorithms built equations for velocities and other measurements (Ranjbar-Karami et al., 2014; Zhang et al., 2020). The intelligent methods have better accuracy but need enough measurements to train the system, moreover the intelligent systems are complex and therefore not easy to build. These features limit extrapolation and application of intelligent methods.

### 2.2. Rock-physics models for S-wave velocity calculation

A rock-physics model describes microstructure and models its effect on the integral properties of rock. For isotropic medium, wave velocities can be calculated by using its bulk modulus ($K$), shear modulus ($\mu$) and density ($\rho$):

$$V_p = \sqrt{\frac{K + \frac{4}{3}\mu}{\rho}} \tag{4}$$

$$V_s = \sqrt{\frac{\mu}{\rho}} \tag{5}$$

Many rock-physics models can provide modulus of rock. In inclusion theory, components of rock are assumed as ellipsoid with different aspect ratios. Components of rock, including minerals and pores, are mixed together homogeneously in SCM (Berryman, 1980). The equations of SCM are:

$$\sum_{i=1}^{N} f_i (K_i - K_{SC}) P_i = 0 \tag{6}$$

$$\sum_{i=1}^{N} f_i (\mu_i - \mu_{SC}) Q_i = 0 \tag{7}$$

where $i$ indicates a component; $f_i$, $K_i$ and $\mu_i$ are volume fraction, bulk modulus and shear modulus of each component, respectively; $K_{SC}$ and $\mu_{SC}$ are effective modulus; $P_i$ and $Q_i$ are geometric factors that are related to modulus and the aspect ratio of each component. Guo and Li (2015) used SCM to predict $V_s$ of the Barnett shale formation, in which volume fractions, modulus and aspect ratios of components are necessary. The aspect ratio of minerals are usually regarded as constants and valued based on former researches (Jiang and Spikes, 2013). But pores have varying aspect ratios which greatly affect modulus. To estimate modulus of rock, the inversion of pore aspect ratios is necessary. The DEM is another inclusion theory, in which inclusions are added to the matrix in sequence (Norris, 1985). To get modulus of rock by DEM, the information used in SCM is required. Ruiz and Dvorkin (2010) used DEM to predict $V_s$. In the inclusion theory, volume fractions, modulus and geometry of components are required to calculate $V_s$. These properties of rock are not easy to get for conventional well logging, especially for the wells without core data.
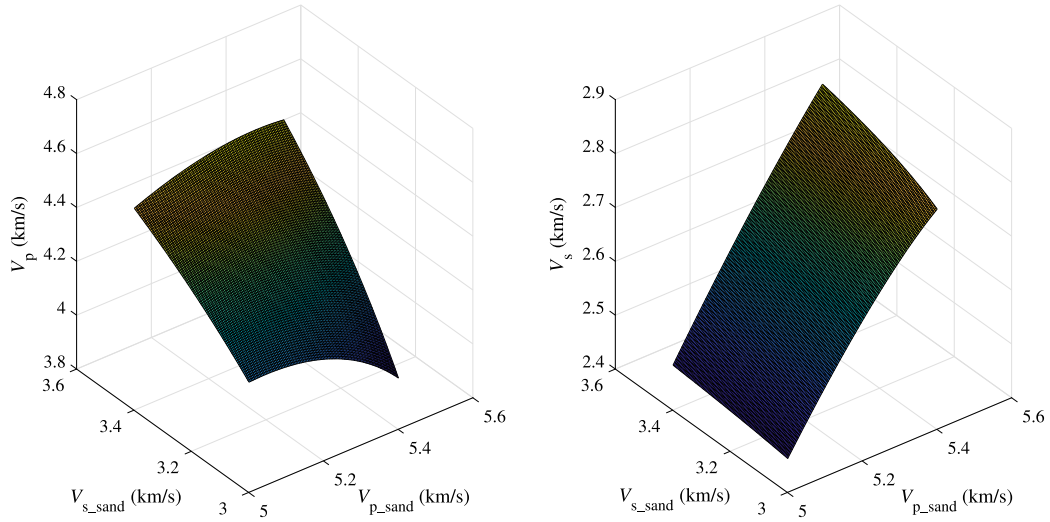
**Fig. 1.** Modeled P- and S-wave velocities of rock with different velocities of sand ($V_{p\_sand}$ and $V_{s\_sand}$) in Xu–White model.
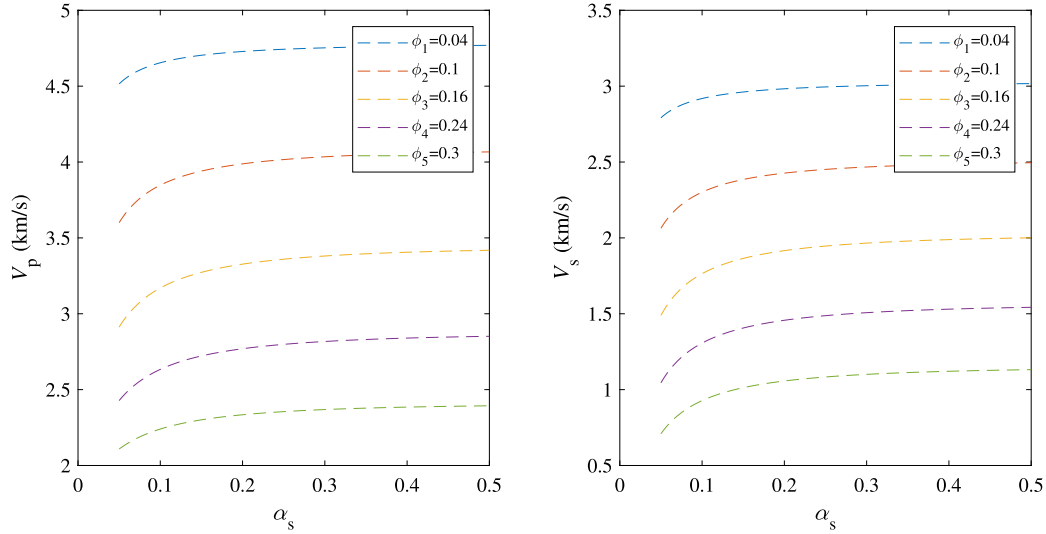


**Fig. 2.** Modeled P- and S-wave velocities with different aspect ratios of sand-related pores in Xu–White model. The rock is made up by quartz, clay and pores. The volume fraction of clay is 0.4.

The Xu–White model can be used to calculate $V_s$. In Xu–White model, matrix is made up by sand and clay, and pores are divided into sand-related pores and clay-related pores:

$$\phi = \phi_s + \phi_c \tag{8}$$

$$\phi_s = f_s \frac{\phi}{1-\phi} \tag{9}$$

$$\phi_c = f_c \frac{\phi}{1-\phi} \tag{10}$$

where $\phi$ indicates porosity, $\phi_s$ indicates sand-related porosity and $\phi_c$ indicates clay-related porosity. Minerals are divided into sand and clay whose volume fractions are indicated by $f_s$ and $f_c$, and $f_s+f_c = 1$. Pores are added into the matrix by using DEM. Keys and Xu (2002) proposed an approximation to avoid the differential computation of DEM. The equations for bulk modulus ($K_d$) and shear modulus ($\mu_d$) of dry rock are:

$$K_d = K_0 (1-\phi)^p \tag{11}$$

$$\mu_d = \mu_0 (1-\phi)^q \tag{12}$$

where $K_0$ and $\mu_0$ are modulus of the matrix. Details of $K_0$, $\mu_0$, $p$ and $q$ are presented in Appendix B. Then the Gassmann's equations

(Gassmann, 1951) are used for fluid saturated rock:

$$K = K_d + \frac{\left(1 - \frac{K_d}{K_0}\right)^2}{\frac{\phi}{K_f} + \frac{(1-\phi)}{K_0} - \frac{K_d}{K_0^2}} \tag{13}$$

$$\mu = \mu_d \tag{14}$$

where $K_f$ is bulk modulus of fluid saturated rock. Density of rock is given by:

$$\rho = (1-\phi)\rho_0 + \phi\rho_f \tag{15}$$

$$\rho_0 = f_s\rho_{sand} + f_c\rho_{clay} \tag{16}$$

$$\rho_f = (1-S_w)\rho_{gas} + S_w\rho_{water} \tag{17}$$

where $\rho_0$ and $\rho_f$ are densities of the matrix and saturated pores; $\rho_{sand}$, $\rho_{clay}$, $\rho_{gas}$ and $\rho_{water}$ are densities of sand, clay, gas and water, respectively; $S_w$ is water saturation.

Given volume fractions, modulus and densities of sand, clay and pores, together with aspect ratio of sand-related pores ($\alpha_s$) and aspect ratio of clay-related pores ($\alpha_c$), modulus of rock can be calculated by Xu–White model. Then velocities are transformed by Eqs. (4) and (5).
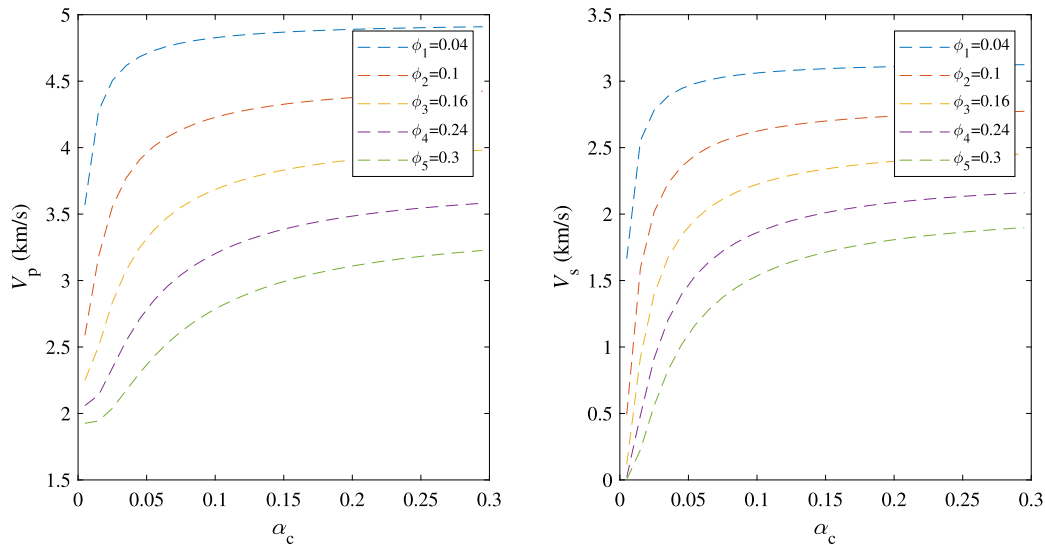
**Fig. 3.** Modeled P- and S-wave velocities with different aspect ratios of clay-related pores in Xu–White model. The rock is made up by quartz, clay and pores. The volume fraction of clay is 0.4.

### 2.3. Predict S-wave velocity for the well

Laboratory experiments provide abundant details of rock, but well-logging data usually only contains some properties, including velocities, density, porosity, clay content and water saturation. Data-based methods seek direct relationships between velocities and other well logs.

More details of rock are required to predict $V_s$ for the well using rock-physics model. Because types and geometry of components affect the integral modulus of rock. Modulus and densities of minerals and fluids are provided by former researches or experiments. In SCM (Eqs. (6) and (7)), volume fractions and aspect ratios of all components are necessary to get effective modulus of rock, since minerals and pores are all mixed together in the model. In DEM, minerals and pores, also called inclusions, are added into the matrix. Volume fractions and aspect ratios of inclusions are required in the process. One option for DEM is building a matrix mixed by all minerals. Some mixing laws allow calculating modulus of the matrix without considering geometry of minerals, such as Hill's average (Hill, 1952):

$$M_H = \frac{1}{2}\left(\sum_{i=1}^N f_i M_i + \frac{1}{\sum_{i=1}^N \frac{f_i}{M_i}}\right)$$ (18)

where $i$ indicates a mineral; $M$ and $f$ are corresponding modulus and volume fractions, respectively; $M_H$ is Hill's effective modulus. In Xu–White model, modulus of the matrix are given by Eqs. (B.1)–(B.4). The mixing law, such as Hill's average, also can be used for the matrix. But in the method, minerals must be identified to get their properties and volume fractions. It is not easy for most wells because conventional logging cannot provide accurate information of minerals (Tan et al., 2015).

In Xu–White model, minerals of sand cannot be identified clearly by conventional well logs, especially for shale. Density of sand can be estimated by Eqs. (15)–(17), but velocities of sand are necessary to get its modulus. Previous researches reported that modulus of sand and clay in the model are constants valued from both experiments and experience (Xu and White, 1996; Bai et al., 2013). The simplification assumes properties of sand and clay do not change with depth. It makes the calculation of rock velocities possible without mineral information. Modeled velocities of rock with different velocities of sand are presented in Fig. 1. It indicates that velocities of rock are affected by velocities of sand in Xu–White model. The simplification of sand properties will lead to errors in $V_s$ prediction.

The aspect ratio of pores seriously affect modulus of rock. Aspect ratios vary with depth and also cannot be measured except experiment (Ruiz and Dvorkin, 2010). Porosity and aspect ratio are regarded as major factors in Xu–White model. Pores are divided into two parts because the property of sand-related pores and clay-related pores are very different. Clay particles tend to form pores with small aspect ratio (Xu and White, 1995). It has been reported that aspect ratio of the two type pores are assumed as constants. The constants of $\alpha_s$ vary from 0.1 to 0.2 and $\alpha_c$ vary from 0.03 to 0.04 (Xu and White, 1995, 1996; Sams and Andrea, 2001; Bai et al., 2013). Figs. 2 and 3 show modeled velocities with different sand-related pores and clay-related pores in Xu–White model. In Fig. 2, $\alpha_s$ is assigned from 0.05 to 0.5, and $\alpha_c$ is 0.04. In Fig. 3, $\alpha_c$ is assigned from 0.005 to 0.3, and $\alpha_s$ is 0.1. The two figures tell $\alpha_s$ and $\alpha_c$ affect velocities of rock in Xu–White model, and velocities are less sensitive to $\alpha_s$. Scholars proposed equations for $\alpha_s$ and porosity (Sams and Andrea, 2001; Pillar et al., 2007). One of them is:

$$\alpha_s = 0.17114 - 0.24477\phi + 0.004314 f_s$$ (19)

The equation can be used to estimate $\alpha_s$. Clay-related pores have small aspect ratios, which have more effect on modulus of rock. Bai et al. (2013) inversed $\alpha_c$ by matching modeled $V_p$ and real data, during which $\alpha_s$ is estimated by Eq. (19). The two parameters are then used in Xu–White model to predict $V_s$. Yan et al. (2002) built a semi-empirical equation to predict velocities by combing Xu–White model and Han's equation. One characteristic of their work is that P- and S-wave velocities of wells are required when building the equation, and then the equation can be used to estimate $V_s$ for other wells. Besides, the equation will work better when the wells are in the same area.

The researches of $V_s$ prediction based on Xu–White model provide better result than empirical methods. Comparing with inclusion theory, details of minerals are ignored and more attention is paid to properties of pores in Xu–White model. This characteristic reduces the dependence on real data. Therefore, Xu–White model is commonly used in $V_s$ prediction.

### 2.4. A statistical rock-physics model for S-wave velocity prediction of wells

Both data-based methods and rock-physics models should be calibrated by real data before they are used to estimate velocities. Real data is collected from well logs and cores or from prior information in previous researches. Certain petrophysical parameters in empirical

equations or rock-physics models are valued by transforming prior information into constants. However, prior information is more likely to form distributions instead of constants, because each parameter has different values under different conditions.

The statistical rock-physics model has been used in reservoir characterization (Bachrach, 2006; Grana and Della Rossa, 2010; Yuan et al., 2016; Fjeldstad and Grana, 2018). In these researches, distributions of key petrophysical parameters are built by prior information and used in the inversion process. Significantly, besides better result, statistical information of the result is provided.

We build a statistical rock-physics model to predict $V_s$ of wells. The Xu–White model acts as a foundation in the statistical model, and prior information is combined to form distributions of key petrophysical parameters. These parameters cannot be measured in well logging and affect velocities of rock in Xu–White model. From Section (2.3), velocities of sand and $\alpha_c$ are important parameters to velocities of rock in Xu–White model. Eq. (19) is utilized to estimate $\alpha_s$, because velocities are less sensitive to $\alpha_s$. Other parameters in the model are available from well logs. By initializing the statistical rock-physics model with distributions from prior information instead of constants, more possibilities are provided to model real velocities of rock with less information.

Prior information is necessary to build the prior distribution for the three key parameters. Data-based methods use real data from well logs and experiments, including part of the target well and several wells in the target area, to get coefficients of equations. These equations are then used to calculate velocities of other part of the target well or other wells in the target area (Han et al., 1986; Yan et al., 2002; Dvorkin and Mavko, 2014; Zhang et al., 2020). A similar approach is utilized in our study. Some wells of target area provide data to form prior distribution of key parameters, which are named reference wells. Then the prior distribution is used to calculate velocities of other wells in the same area, which are named target wells. The reference well has accurate and abundant data, including mineral information. Velocities of sand in reference wells can be calculated by using mixing theory Eq. (18). $\alpha_s$ of reference wells is estimated by Eq. (19). The following equation is the objective function for $\alpha_c$ inversion of reference wells:

$$\alpha_c = \arg\ \min\left(\left|\frac{\widetilde{V_p} - V_p}{V_p}\right| + \left|\frac{\widetilde{V_s} - V_s}{V_s}\right|\right) \tag{20}$$

where $\widetilde{V_p}$ and $\widetilde{V_s}$ are modeled P- and S-wave velocities by Xu–White model.

The prior distribution and $V_p$ of the target well are used in the inversion of P-wave velocity of sand ($V_{p\_sand}$), S-wave velocity of sand ($V_{s\_sand}$) and $\alpha_c$ of the target well. $\alpha_s$ of the target well is provided by Eq. (19). The Bayesian inversion framework can combine prior information with statistical model in the inversion process, and has been used in geophysical inversion problems (Mollajan et al., 2019a,b). We use Bayesian theory to process the inversion and the objective function is:

$$\boldsymbol{m} = \arg\ \max\left(P\left(\boldsymbol{m}|V_p\right)\right) \tag{21}$$

$$P\left(\boldsymbol{m}|V_p\right) \propto P\left(V_p|\boldsymbol{m}\right) P\left(\boldsymbol{m}\right) = N\left(V_p; \widetilde{V_p}, \mathbf{V_1}\right) N\left(\boldsymbol{m}; \mathbf{E}, \mathbf{V_2}\right) \tag{22}$$

where $\boldsymbol{m}$ is a vector made up by the three parameters; $P\left(\cdot\right)$ is the probability function; $N\left(\cdot\right)$ is the probability of a normal distribution; $\mathbf{V_1}$ is the variance of noise in $V_p$; $\mathbf{E}$ is a vector made up by expectations of the three parameters and $\mathbf{V_2}$ is the covariance matrix.

To solve non-linear objective function in inversion problems, the global optimization algorithm is a choice (Liu and Grana, 2018). The SA-PSO is a particle swarm optimization algorithm improved by simulated annealing. The algorithm has been used to solve nonlinear inversion problems of reservoir characterization (Zhang et al., 2017, 2018b). The SA-PSO is employed here to solve the objective function (Eq. (21)). The algorithm searches for best values of the three key parameters ($\boldsymbol{m}$) to make the posterior probability ($P\left(\boldsymbol{m}|V_p\right)$) maximum.
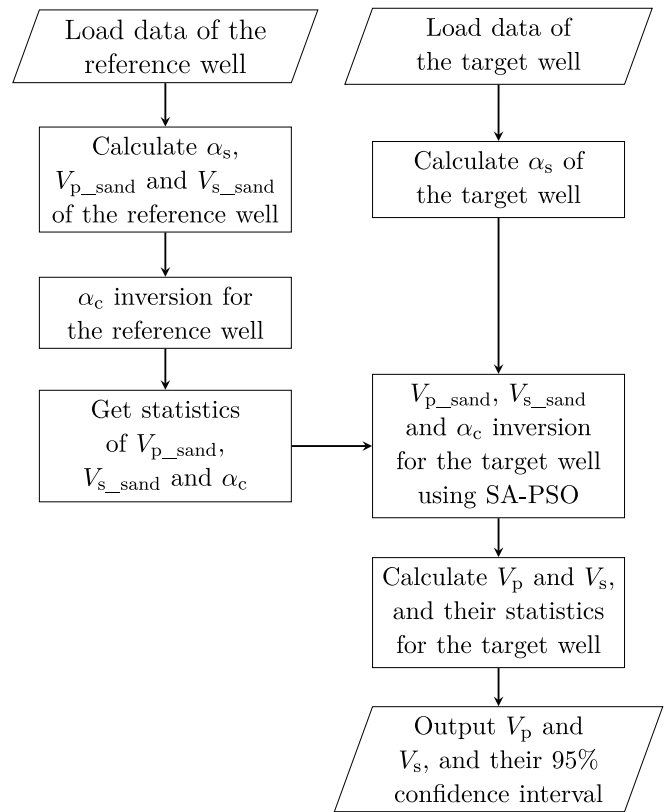


**Fig. 4.** Workflow of S-wave velocity prediction for wells based on statistical rock-physics model and Bayesian theory.

Then the three key parameters are used to calculate $V_s$ of wells based on the rock-physics model. During the process, the statistical method will provide not only the best estimation of $V_s$, but also statistics of the result, such as confidence interval and probability. Fig. 4 is the workflow of $V_s$ prediction for wells based on the statistical rock-physics model and Bayesian theory.

## 3. Results and discussion

A reservoir from South China is chosen for real data test. The reservoir is a shale formation and there are several wells in the area. Two reference wells have mineral information. Fig. 5 is logging curves of a reference well, including gamma ray, $V_p$, $V_s$, density, porosity, water saturation and volume fraction of components. Mineral information is calculated from well logs and core data. Except reference wells, other wells only have conventional logging curves and mineral information is unavailable. We use three of them as target wells, which have real $V_s$ logging data for validation of the method. Fig. 6 is logging curves of target well 1. Well logs of target wells come from the same shale formation with reference wells and thus the properties of rock are similar. Modulus and densities of minerals and fluids of the formation are presented in Table 1.

Firstly, the inversion of $\alpha_c$ is processed for the two reference wells. Velocities of sand are calculated based on mineral information from well logs. Inversion results of the three parameters are presented in Fig. 7. It shows the statistics of reference wells, from which prior distribution is built for the following process.

For the target well, the density of sand is given by Eqs. (15)–(17), and $\alpha_s$ is given by Eq. (19). There are three key parameters in the statistical model to calculate $V_s$ of target wells. The inversion of them is processed by solving the objective function (Eq. (21)) with the prior distribution from reference wells. Then velocities and their
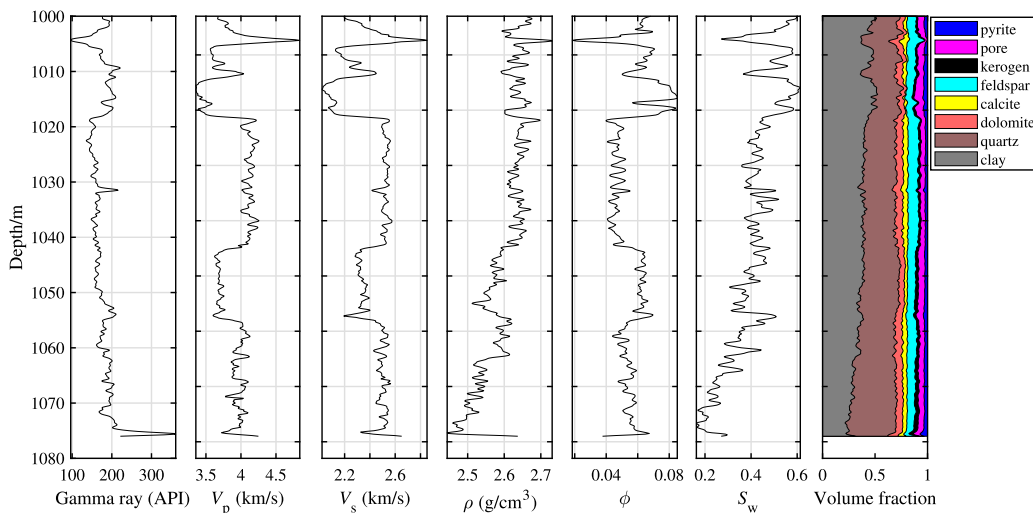
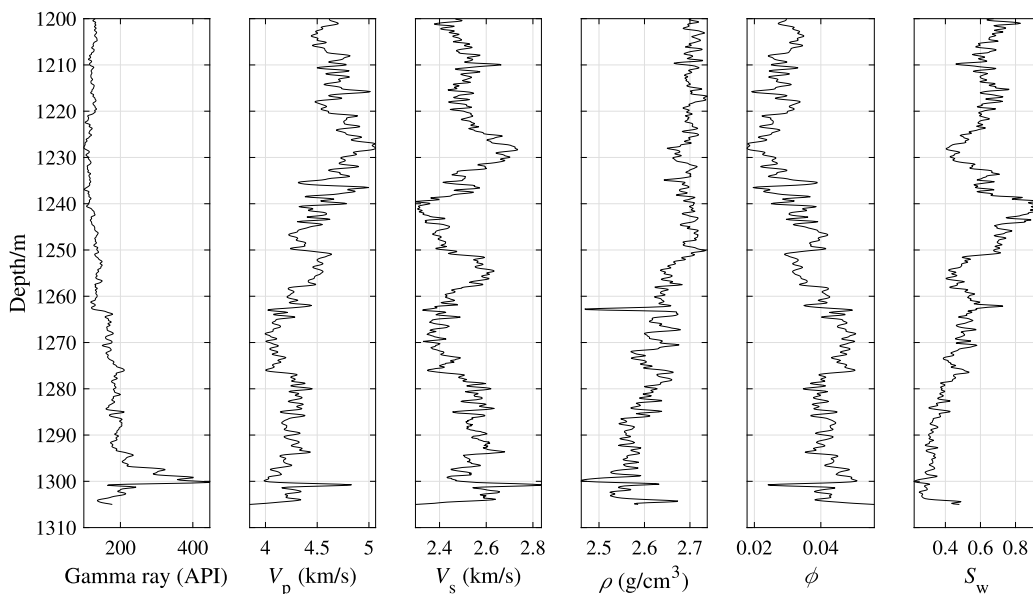**Fig. 5.** Well logs of a reference well with artificial depths.



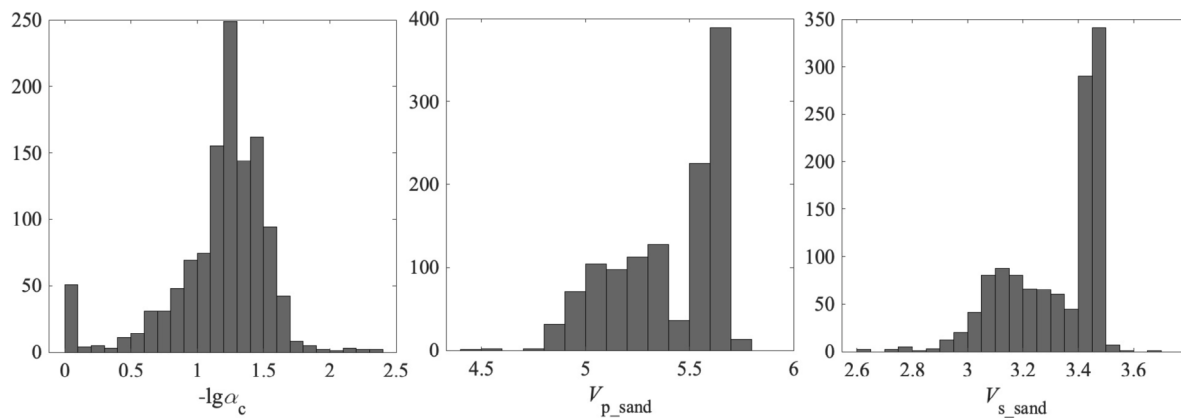**Fig. 6.** Well logs of target well 1 with artificial depths.



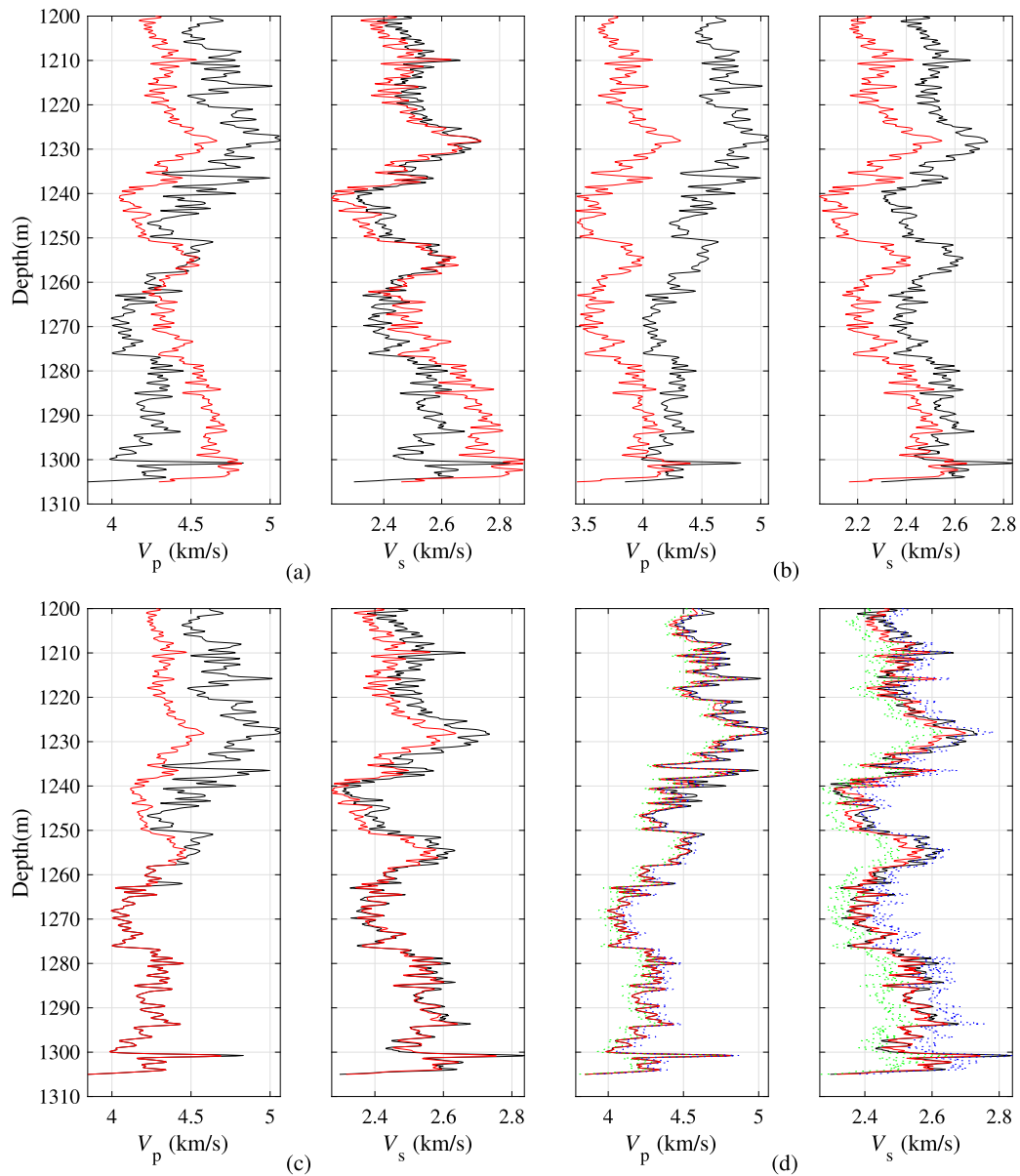**Fig. 7.** Prior information from statistics of reference wells.

**Fig. 8.** Predicted P- and S-wave velocities (red) and real velocities (black) of target well 1. (a) is result of Han's model, (b) is result of the Xu–White model with all constant parameters, (c) is result of the Xu–White model with variable $\alpha_c$ and (d) is result of the statistical model, where green dots and blue dots are the lower boundary and upper boundary of 95% confidence interval, respectively. (For interpretation of the references to color in this figure legend, the reader is referred to the web version of this article.)

**Table 1**
Modulus and densities of minerals and fluids (Mavko et al., 2009; Jiang and Spikes, 2013; Tan et al., 2015).

|  | Bulk modulus (GPa) | Shear modulus (GPa) | Density (g/cm³) |
|---|---|---|---|
| Quartz | 37.9 | 44.3 | 2.65 |
| Dolomite | 94.9 | 45 | 2.87 |
| Calcite | 76.8 | 32 | 2.71 |
| Feldspar | 37.5 | 15 | 2.62 |
| Pyrite | 147.4 | 132.5 | 4.93 |
| Clay | 25 | 9 | 2.55 |
| Kerogen | 2.9 | 2.7 | 1.3 |
| Gas | 0.336 | – | 0.34 |
| Water | 2.2 | – | 1.4 |

statistics are calculated based on the inversion result. As a comparison, Han's model (Han et al., 1986), the Xu–White model with all constant parameters (Xu and White, 1995, 1996) and the Xu–White model with

variable $\alpha_c$ (Bai et al., 2013) are utilized in target wells. These methods are also evaluated quantitatively by MSE and correlation coefficient (*r*). Their equations are:

$$\text{MSE} = \frac{1}{N} \sum_{i=1}^{N} \left( \widetilde{V}_i - V_i \right)^2 \tag{23}$$

$$r = \frac{cov\left( \widetilde{V}, V \right)}{\sigma \widetilde{V} \sigma V} \tag{24}$$

where *i* indicates depth points; $\widetilde{V}_i$ and $V_i$ are corresponding estimated velocities and real velocities, respectively; *N* is the total number of depth points; $cov(\cdot)$ indicates covariance and $\sigma$ indicates standard deviation of velocities.

Results of the four methods for target well 1 are shown in Fig. 8. And quantitative evaluation of these methods are presented in Table 2. It is obvious that the three old methods get results with different errors. The Xu–White model based methods have higher correlation
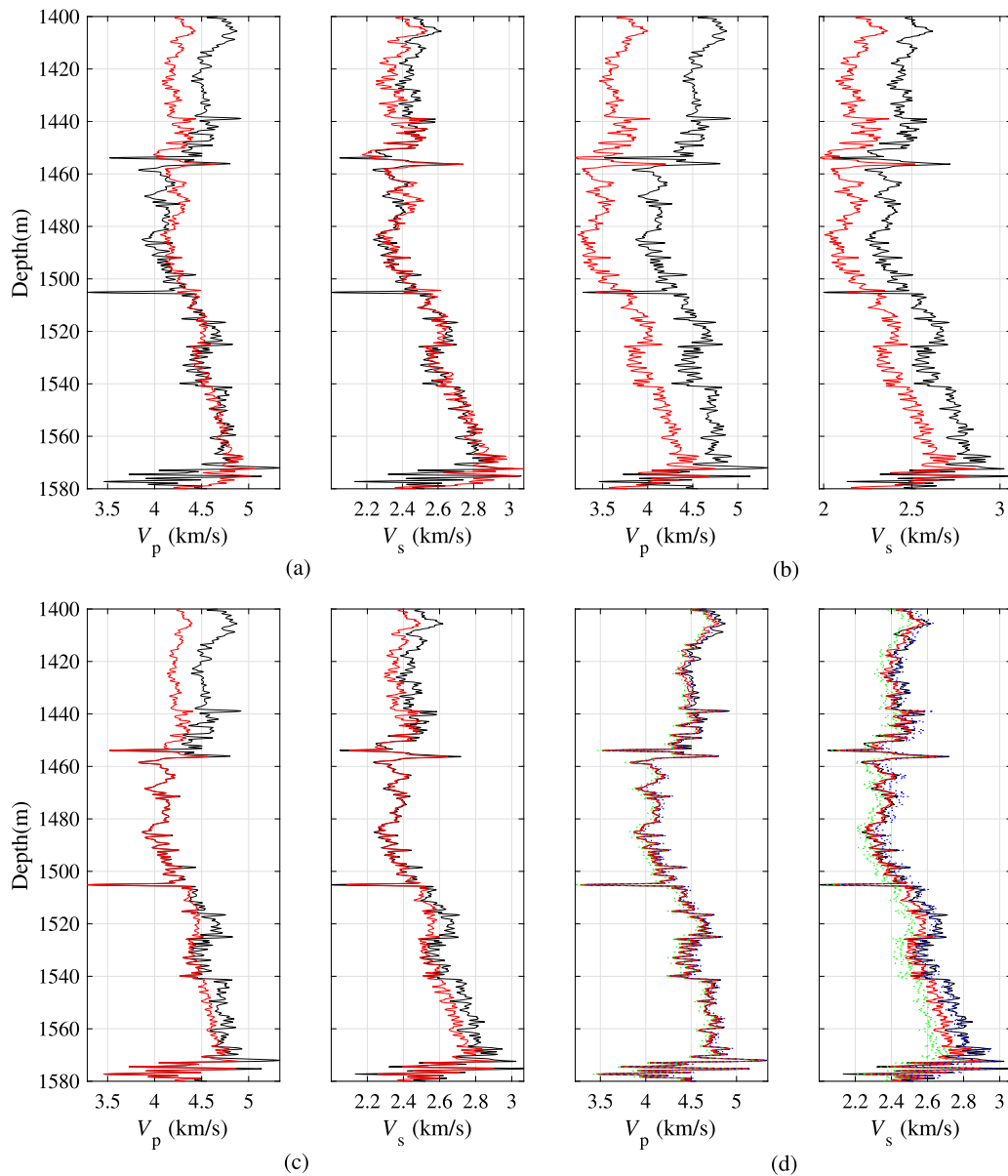
**Fig. 9.** Predicted P- and S-wave velocities (red) and real velocities (black) of target well 2. (a) is result of Han's model, (b) is result of the Xu–White model with all constant parameters, (c) is result of the Xu–White model with variable $\alpha_c$ and (d) is result of the statistical model, where green dots and blue dots are the lower boundary and upper boundary of 95% confidence interval, respectively. (For interpretation of the references to color in this figure legend, the reader is referred to the web version of this article.)

**Table 2**
The comparison of mean square error (MSE) and correlation coefficient ($r$) of predicted $V_p$ and $V_s$ using different models.

|  | Model | MSE of $V_p$ | MSE of $V_s$ | $r$ of $V_p$ | $r$ of $V_s$ |
|---|---|---|---|---|---|
| Target well 1 | Han's model | 0.1084 | 0.0115 | −0.1322 | 0.7264 |
|  | Xu–White model (constants) | 0.4421 | 0.0411 | 0.3854 | 0.8444 |
|  | Xu–White model (variable $\alpha_c$) | 0.0602 | 0.0030 | 0.7954 | 0.9128 |
|  | Statistical model | 0.0019 | 0.0012 | 0.9966 | 0.9433 |
| Target well 2 | Han's model | 0.0648 | 0.0073 | 0.5315 | 0.8872 |
|  | Xu–White model (constants) | 0.4753 | 0.0554 | 0.7498 | 0.9341 |
|  | Xu–White model (variable $\alpha_c$) | 0.0419 | 0.0047 | 0.8592 | 0.9699 |
|  | Statistical model | 0.0015 | 0.0030 | 0.9958 | 0.9864 |
| Target well 3 | Han's model | 0.0540 | 0.0068 | 0.6470 | 0.9571 |
|  | Xu–White model (constants) | 0.7479 | 0.0872 | 0.7867 | 0.9788 |
|  | Xu–White model (variable $\alpha_c$) | 0.0514 | 0.0049 | 0.7693 | 0.9664 |
|  | Statistical model | 0.0017 | 0.0018 | 0.9952 | 0.9868 |

than Han's model considering the last three methods are based on Xu–White model. But the two old Xu–White model based methods have bigger error than Han's model, at least in some sections. The reason is that Han's model is built by data fitting and thus has smaller global error. But in special sections the error becomes big. Even the trends of estimated and real velocities are converse, such as the section from 1285 to 1300 in Fig. 8a. In Fig. 8b, constant parameters are used in Xu–White model and there is big error in the result. Because some key parameters, such as $V_{p\_sand}$ and $\alpha_c$, are assigned based on knowledge of reference wells and not accurate for the target well. Besides, properties of rock vary with depth, therefore constant parameters lead errors. Fig. 8c gives better result than Fig. 8b. And the MSE as well as $r$ is improved. The reason is that $\alpha_c$ is from inversion and $\alpha_s$ is calculated from porosity and volume fraction of sand (Eq. (19)) in the method. The two parameters are important to velocities of rock (Figs. 2 and 3), therefore the accuracy of the two parameters improves the result. But there are still big errors between estimation and real data in some sections, such as 1200 to 1230 in Fig. 8c. The statistical method
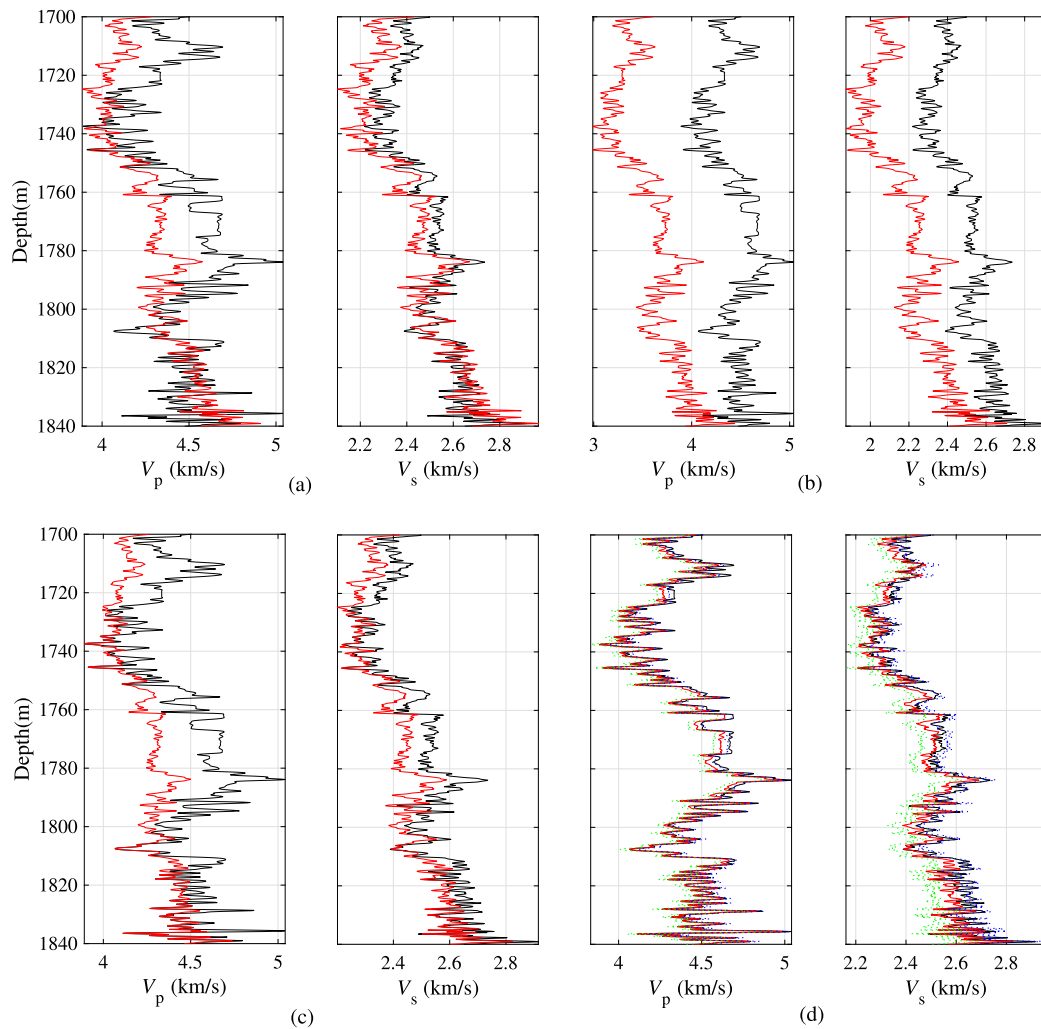
Fig. 10. Predicted P- and S-wave velocities (red) and real velocities (black) of target well 3. (a) is result of Han's model, (b) is result of the Xu–White model with all constant parameters, (c) is result of the Xu–White model with variable $\alpha_c$ and (d) is result of the statistical model, where green dots and blue dots are the lower boundary and upper boundary of 95% confidence interval, respectively. (For interpretation of the references to color in this figure legend, the reader is referred to the web version of this article.)

achieves the best result. In Fig. 8d, predicted $V_p$ and $V_s$ are fitting well with real velocities. Errors of the result are small in no matter global or special sections. The trends of estimation and real data are similar, which are indicated by $r$. The result is achieved by the inversion of three key parameters using Bayesian theory, which is more effective than the single $\alpha_c$ inversion in Fig. 8c. Moreover, the 95% confidence interval is provided in Fig. 8d and real velocities are in the interval. Also note that the confidence interval is narrow, which limits the range of real velocities. The results in Fig. 8 indicate that the statistical method can provide not only accurate velocity estimation for wells, but also a valuable small range which the real velocity is almost in.

To test the applicability of the statistical method, target well 2 and target well 3 are also used in the workflow. The results are shown in Figs. 9 and 10, and their quantitative evaluation is presented in Table 2. The two well tests demonstrate a similar result with target well 1 and validate the statistical method.

As prior information is required in the workflow, reference wells with abundant logging and core data are necessary for the method. Prior information also affects accuracy of the velocity estimation. Sections of target wells should be similar with reference wells to guarantee that the prior information is correct and the result will be best. The method is still valid for a longer logging interval in target wells, because velocities are also determined by the fitting of real $V_p$ besides prior information. But accuracy of the result will decrease when the depth

is far away from the section which is similar with reference wells. The reference wells and target wells are in a same reservoir in this study to ensure similar rock properties, which also improves prior information. Reference wells from the similar reservoir can also provide the prior information but its validity and accuracy should be verified at first, and accuracy of the result will decrease.

## 4. Conclusions

In this study, a statistical method is proposed to predict $V_s$ of wells. This method is based on a statistical rock-physics model and Bayesian inversion theory. The details of building a statistical rock-physics model is presented, and the workflow of the statistical method is summarized. This method is suitable to predict $V_s$ for wells in a reservoir, where only few wells have abundant logging and core data, and is also applicable to an area where there are only conventional well logs. The application of this method will contribute to AVO analysis and reservoir characterization.

Real data tests and results indicate that the method can provide accurate $V_s$ prediction. The statistics of the estimation are also presented, from which the 95% confidence interval of estimated velocities is calculated. The confidence interval is proved valid by comparing with real velocities. Furthermore, $V_s$ of wells, as well as $V_p$, has been utilized

as calibration for statistical inversion of petrophysical parameters of reservoirs in recent years. The statistical information and accurate velocities are valuable to these researches.

## CRediT authorship contribution statement

**Bing Zhang:** Conceptualization, Methodology, Software, Validation, Writing - original draft, Writing - review & editing. **Shuanggen Jin:** Resources, Writing - review & editing, Project administration, Acquisition of the financial support for the project leading to this publication. **Cai Liu:** Supervision, Resources. **Zhiqi Guo:** Resources, Software. **Xiwu Liu:** Resources, Data curation.

## Declaration of competing interest

The authors declare that they have no known competing financial interests or personal relationships that could have appeared to influence the work reported in this paper.

## Acknowledgments

## Appendix A. Abbreviations and their explanation

Some abbreviations and their explanation in this paper are listed below. The units of symbols are also provided.

| | | |
|---|---|---|
| $V_s$ or S-wave velocity | Shear wave velocity | km/s |
| $V_p$ or P-wave velocity | Compression wave velocity | km/s |
| AVO | Amplitude variation with offset | |
| SCM | The self-consistent model | |
| DEM | The differential effective medium model | |
| $\phi$ | Porosity | |
| $C$ | Volume fraction of clay content in a rock | |
| $K$ | Bulk modulus | GPa |
| $\mu$ | Shear modulus | GPa |
| $\rho$ | Density | g/cm$^3$ |
| $\phi_s$ | Sand-related porosity | |
| $\phi_c$ | Clay-related porosity | |
| $f_s$ | Volume fraction of sand in minerals which constitute a rock | |
| $f_c$ | Volume fraction of clay in minerals which constitute a rock | |
| $K_d$ | Bulk modulus of dry rock | GPa |
| $\mu_d$ | Shear modulus of dry rock | GPa |
| $S_w$ | Water saturation | |
| $\alpha$ | Aspect ratio | |
| $\alpha_s$ | Aspect ratio of sand-related pores | |
| $\alpha_c$ | Aspect ratio of clay-related pores | |
| $V_{s\_sand}$ | Shear wave velocity of sand | km/s |
| $V_{p\_sand}$ | Compression wave velocity of sand | km/s |
| SA-PSO | Particle swarm optimization algorithm improved by simulated annealing | |
| MSE | Mean square error of an array | |
| $r$ | Correlation coefficient of two arrays | |

## Appendix B. Extend equations of Xu–White model

Xu and White (1995, 1996) gave equations for modulus of the matrix, which is made up by sand and clay, by the time-average:

$$T_0^P = \left(1 - f_c'\right) T_s^P + f_c' T_c^P \tag{B.1}$$

$$T_0^S = \left(1 - f_c'\right) T_s^S + f_c' T_c^S \tag{B.2}$$

$$K_0 = \rho_0 \left( \frac{1}{\left(T_0^P\right)^2} + \frac{4}{3 \left(T_0^S\right)^2} \right) \tag{B.3}$$

$$\mu_0 = \rho_0 \left( \frac{1}{\left(T_0^S\right)^2} \right) \tag{B.4}$$

where $T_0^P$, $T_s^P$ and $T_c^P$ are P-wave transit times of the matrix, sand and clay, respectively; $T_0^S$, $T_s^S$ and $T_c^S$ are S-wave transit times of the matrix, sand and clay, respectively; $K_0$ and $\mu_0$ are modulus of the matrix; The transit times are reciprocals of velocities; $f_c'$ is the normalized clay volume fraction and $\rho_0$ is density of the matrix, which are calculated by:

$$f_c' = \frac{f_c}{1 - \phi} \tag{B.5}$$

$$\rho_0 = \left(1 - f_c'\right) \rho_s + f_c' \rho_c \tag{B.6}$$

$\rho_s$ and $\rho_c$ are density of sand and clay, respectively.

In Eqs. (11) and (12), $p$ and $q$ are geometry coefficients which are functions of aspect ratio:

$$p = \frac{1}{3} \sum_{l=S,C} f_l T_{iijj}\left(\alpha_l\right) \tag{B.7}$$

$$q = \frac{1}{5} \sum_{l=S,C} f_l F\left(\alpha_l\right) \tag{B.8}$$

S and C indicate sand and clay; $\alpha$ is the aspect ratio of corresponding pores and $f$ indicates corresponding volume fraction. Equations for $T_{iijj}(\alpha)$ and $F(\alpha)$ are given by (Berryman, 1980):

$$T_{iijj}(\alpha) = \frac{3F_1}{F_2} \tag{B.9}$$

$$F(\alpha) = \frac{2}{F_3} + \frac{1}{F_4} + \frac{F_4 F_5 + F_6 F_7 - F_8 F_9}{F_2 F_4} \tag{B.10}$$

where

$$F_1 = 1 + A \left[ \frac{3}{2}(g+v) - R\left(\frac{3}{2}g + \frac{5}{2}v - \frac{4}{3}\right) \right] \tag{B.11}$$

$$F_2 = 1 + A \left[ 1 + \frac{3}{2}(g+v) - \frac{R}{2}(3g+5v) \right] + B(3-4R)$$
$$\quad + \frac{A}{2}[A+3B](3-4R)\left[ g + v - R\left(g - v + 2v^2\right) \right] \tag{B.12}$$

$$F_3 = 1 + \frac{A}{2} \left[ R(2-v) + \frac{1+\alpha^2}{\alpha^2} g(R-1) \right] \tag{B.13}$$

$$F_4 = 1 + \frac{A}{4} [3v + g - R(g-v)] \tag{B.14}$$

$$F_5 = A \left[ R\left(g + v - \frac{4}{3}\right) - g \right] + Bv(3-4R) \tag{B.15}$$

$$F_6 = 1 + A[1 + g - R(v+g)] + B(1-v)(3-4R) \tag{B.16}$$

$$F_7 = 2 + \frac{A}{4}[9v + 3g - R(5v+3g)] + Bv(3-4R) \tag{B.17}$$

$$F_8 = A \left[ 1 - 2R + \frac{g}{2}(R-1) + \frac{v}{2}(5R-3) \right] + B(1-v)(3-4R) \tag{B.18}$$

$$F_9 = A[g(R-1) - Rv] + Bv(3-4R) \tag{B.19}$$

and $A = \frac{\mu'}{\mu} - 1$, $B = \frac{1}{3}\left(\frac{K'}{K} - \frac{\mu'}{\mu}\right)$, $R = \frac{3\mu}{3K+4\mu}$, $g = \frac{\alpha^2}{1-\alpha^2}(3v-2)$, $v = \frac{\alpha}{(1-\alpha^2)^{\frac{3}{2}}}\left[\cos^{-1}(\alpha) - \alpha\sqrt{1-\alpha^2}\right]$. $K$ and $\mu$ are bulk modulus and shear modulus of the matrix, respectively. $K'$, $\mu'$ and $\alpha$ are bulk modulus, shear modulus and aspect ratio of the inclusion, respectively.

## Appendix C. The SA-PSO algorithm

The SA-PSO is a particle swarm optimization algorithm improved by simulated annealing. The algorithm can search optimal solution of inversion parameters in a non-linear function. The workflow of SA-PSO is as follow:

1. Initialization. Samples are drawn from the solution space randomly to get particles.

$$x_0^i \sim U(S) \tag{C.1}$$

$$\upsilon_0^i \sim U(s) \tag{C.2}$$

$$s = \left[0, \frac{1}{2}\left(S_u - S_d\right)\right] \tag{C.3}$$

where $x_0^i$ and $\upsilon_0^i$ are initial position and initial velocity of particle $i$, respectively. A particle has dimensionality and each dimensionality represents an inversion parameter. So, the position of a particle represents the values of inversion parameters. In these functions, $U$ refers sampling with equal probability, and $S$ is the solution space of the inversion parameters with upper boundary $S_u$ and lower boundary $S_d$. The initial space of velocity is $s$ which is decided by the solution space. The temperature for the annealing process is $T_0$, which should be a big enough constant.

2. Calculate the fitness of particles.

$$fit\left(x_k^i\right) = f\left(x_k^i\right) \tag{C.4}$$

where $fit$ is the fitness of particles; $f$ is the objective function; $x_k^i$ is the position of particle $i$ in cycle $k$.

3. Change the position of particles.

$$\upsilon_{k+1}^i = \upsilon_k^i + c_1 r_1 \left(p_i - x_k^i\right) + c_2 r_2 \left(p_g - x_k^i\right) \tag{C.5}$$

$$x_{temp}^i = x_k^i + \upsilon_{k+1}^i \tag{C.6}$$

where $c_1$ and $c_2$ are constants; $r_1$ and $r_2$ are valued randomly between 0 and 1; $\upsilon_k^i$ is the velocity of particle $i$ in cycle $k$, and $\upsilon_{k+1}^i$ is its velocity in cycle $k+1$; $p_g$ is the global-best, which is the position of particle whose fitness is biggest in all particles till now; $p_i$ is the individual-best, which is the position of the particle where its fitness is biggest till now; $x_{temp}^i$ is a possible position where the particle might be after this cycle, and it is decided by the two equations:

$$fit\left(x_{temp}^i\right) > fit\left(x_k^i\right) \tag{C.7}$$

$$exp\left(\frac{-\left(fit\left(x_{temp}^i\right) - fit\left(x_k^i\right)\right)}{T_k}\right) > r_3 \tag{C.8}$$

where $r_3$ is valued randomly between 0 and 1. Particles will move if they meet at least one of these equations. That is $x_{k+1}^i = x_{temp}^i$. Otherwise particles will not move.

4. Lower the temperature.

$$T_{k+1} = cT_k \tag{C.9}$$

where $c$ is a coefficient of the operation.

5. Repeat steps 2 to 4 until the condition of convergence is meet. Then, $p_g$ is the optimal solution for the function.

## References

Asoodeh, M., Bagheripour, P., 2012. Prediction of compressional, shear, and stoneley wave velocities from conventional well log data using a committee machine with intelligent systems. Rock Mech. Rock Eng. 45 (1), 45–63. http://dx.doi.org/10.1007/s00603-011-0181-2.

Bachrach, R., 2006. Joint estimation of porosity and saturation using stochastic rock-physics modeling. Geophysics 71 (5), O53–O63. http://dx.doi.org/10.1190/1.2235991.

Bai, J.-Y., Yue, C.-Q., Liang, Y.-Q., Song, Z.-X., Ling, S., Zhang, Y., Wu, W., 2013. Variable aspect ratio method in the Xu–White model for shear-wave velocity estimation. J. Geophys. Eng. 10 (3), 035008. http://dx.doi.org/10.1088/1742-2132/10/3/035008.

Berryman, J.G., 1980. Long-wavelength propagation in composite elastic media II. Ellipsoidal inclusions. J. Acoust. Soc. Am. 68 (6), 1820–1831. http://dx.doi.org/10.1121/1.385172.

Castagna, J.P., Backus, M.M., 1993. Offset-dependent reflectivity—Theory and practice of AVO analysis. In: Castagna, J.P., Backus, M.M. (Eds.), Investigations in Geophysics. Society of Exploration Geophysicists, http://dx.doi.org/10.1190/1.9781560802624.

Castagna, J.P., Batzle, M.L., Eastwood, R.L., 1985. Relationships between compressional-wave and shear-wave velocities in clastic silicate rocks. Geophysics 50 (4), 571–581. http://dx.doi.org/10.1190/1.1441933.

Dvorkin, J., Mavko, G., 2014. Vs predictors revisited. Lead. Edge 33 (3), 288–296. http://dx.doi.org/10.1190/tle33030288.1.

Fjeldstad, T., Grana, D., 2018. Joint probabilistic petrophysics-seismic inversion based on Gaussian mixture and Markov chain prior models. Geophysics 83 (1), R31–R42. http://dx.doi.org/10.1190/GEO2017-0239.1.

Gassmann, F., 1951. Uber die elastizität poröser medien. Vierteljahresschr. Nat.forsch. Ges. Zür. 96, 1–23.

Grana, D., Della Rossa, E., 2010. Probabilistic petrophysical-properties estimation integrating statistical rock physics with seismic inversion. Geophysics 75 (3), O21–O37. http://dx.doi.org/10.1190/1.3386676.

Guo, Z., Li, X.-Y., 2015. Rock physics model-based prediction of shear wave velocity in the Barnett Shale formation. J. Geophys. Eng. 12 (3), 527–534. http://dx.doi.org/10.1088/1742-2132/12/3/527.

Han, D., Nur, A., Morgan, D., 1986. Effects of porosity and clay content on wave velocities in sandstones. Geophysics 51 (11), 2093–2107. http://dx.doi.org/10.1190/1.1442062.

Hill, R., 1952. The elastic behaviour of a crystalline aggregate. Proc. Phys. Soc. Sect. A 65 (5), 349–354. http://dx.doi.org/10.1088/0370-1298/65/5/307.

Hui, Z., Jin, S., Cheng, P., Ziggah, Y.Y., Wang, L., Wang, Y., Hu, H., Hu, Y., 2019. An active learning method for DEM extraction from airborne LiDAR point clouds. IEEE Access 7, 89366–89378. http://dx.doi.org/10.1109/ACCESS.2019.2926497.

Jia, Y., Jin, S., Savi, P., Gao, Y., Tang, J., Chen, Y., Li, W., 2019. GNSS-R soil moisture retrieval based on a XGboost machine learning aided method: Performance and validation. Remote Sens. 11 (14), http://dx.doi.org/10.3390/rs11141655.

Jiang, M., Spikes, K.T., 2013. Estimation of reservoir properties of the Haynesville Shale by using rock-physics modelling and grid searching. Geophys. J. Int. 195 (1), 315–329. http://dx.doi.org/10.1093/gji/ggt250.

Keys, R.G., Xu, S., 2002. An approximation for the Xu-White velocity model. Geophysics 67 (5), 1406–1414. http://dx.doi.org/10.1190/1.1512786.

Liu, M., Grana, D., 2018. Stochastic nonlinear inversion of seismic data for the estimation of petroelastic properties using the ensemble smoother and data reparameterization. Geophysics 83 (3), M25–M39. http://dx.doi.org/10.1190/geo2017-0713.1.

Mavko, G., Mukerji, T., Dvorkin, J., 2009. The Rock Physics Handbook: Tools for Seismic Analysis of Porous Media, second ed. Cambridge University Press, p. 339.

Mollajan, A., Memarian, H., Quintal, B., 2019a. Imperialist competitive algorithm optimization method for nonlinear amplitude variation with angle inversion. Geophysics 84 (3), N81–N92. http://dx.doi.org/10.1190/geo2018-0507.1.

Mollajan, A., Memarian, H., Quintal, B., 2019b. Sparse Bayesian linearized amplitude-versus-angle inversion. Geophys. Prospect. 67 (7), 1745–1763. http://dx.doi.org/10.1111/1365-2478.12789.

Norris, A., 1985. A differential scheme for the effective moduli of composites. Mech. Mater. 4 (1), 1–16. http://dx.doi.org/10.1016/0167-6636(85)90002-X.

Pillar, N., Yan, J., Lubbe, R., 2007. Variable aspect ratio method in the Xu-White model for AVO. In: 69th EAGE Conference and Exhibition Incorporating SPE EUROPEC 2007. http://dx.doi.org/10.3997/2214-4609.201401648.

Rajabi, M., Bohloli, B., Gholampour Ahangar, E., 2010. Intelligent approaches for prediction of compressional, shear and stoneley wave velocities from conventional well log data: A case study from the Sarvak carbonate reservoir in the Abadan Plain (Southwestern Iran). Comput. Geosci. 36 (5), 647–664. http://dx.doi.org/10.1016/j.cageo.2009.09.008.

Ranjbar-Karami, R., Kadkhodaie-Ilkhchi, A., Shiri, M., 2014. A modified fuzzy inference system for estimation of the static rock elastic properties: A case study from the Kangan and Dalan gas reservoirs, South Pars gas field, the Persian Gulf. J. Nat. Gas Sci. Engineering 21, 962–976. http://dx.doi.org/10.1016/j.jngse.2014.10.034.

Ruiz, F., Dvorkin, J., 2010. Predicting elasticity in nonclastic rocks with a differential effective medium model. Geophysics 75 (1), E41–E53. http://dx.doi.org/10.1190/1.3267854.

Sams, M.S., Andrea, M., 2001. The effect of clay distribution on the elastic properties of sandstones. Geophys. Prospect. 49 (1), 128–150. http://dx.doi.org/10.1046/j.1365-2478.2001.00230.x.

Sohail, G.M., Hawkes, C.D., 2020. An evaluation of empirical and rock physics models to estimate shear wave velocity in a potential shale gas reservoir using wireline logs. J. Pet. Sci. Eng. 185 (November 2019), 106666. http://dx.doi.org/10.1016/j.petrol.2019.106666.

Tan, M., Peng, X., Cao, H., Wang, S., Yuan, Y., 2015. Estimation of shear wave velocity from wireline logs in gas-bearing shale. J. Pet. Sci. Eng. 133, 352–366. http://dx.doi.org/10.1016/j.petrol.2015.05.020.

Vernik, L., Castagna, J., Omovie, S.J., 2018. S-wave velocity prediction in unconventional shale reservoirs. Geophysics 83 (1), MR35–MR45. http://dx.doi.org/10.1190/geo2017-0349.1.

Xu, S., Payne, M.A., 2009. Modeling elastic properties in carbonate rocks. Lead. Edge 28 (1), 66–74. http://dx.doi.org/10.1190/1.3064148.

Xu, S., White, R.E., 1995. A new velocity model for clay-sand mixtures. Geophys. Prospect. 43 (1), 91–118. http://dx.doi.org/10.1111/j.1365-2478.1995.tb00126.x.

Xu, S., White, R.E., 1996. A physical model for shear-wave velocity prediction. Geophys. Prospect. 44 (4), 687–717. http://dx.doi.org/10.1111/j.1365-2478.1996.tb00170.x.

Yan, J., Li, X.-Y., Enru, L., 2002. Effects of pore aspect ratios on velocity prediction from well-log data. Geophys. Prospect. 50 (3), 289–300. http://dx.doi.org/10.1046/j.1365-2478.2002.00313.x.

Yuan, C., Li, J., Chen, X., Rao, Y., 2016. Quantitative uncertainty evaluation of seismic facies classification: A case study from northeast China. Geophysics 81 (3), B87–B99. http://dx.doi.org/10.1190/geo2015-0228.1.

Zhang, D., Lin, J., Peng, Q., Wang, D., Yang, T., Sorooshian, S., Liu, X., Zhuang, J., 2018a. Modeling and simulating of reservoir operation using the artificial neural network, support vector regression, deep learning algorithm. J. Hydrol. 565 (May), 720–736. http://dx.doi.org/10.1016/j.jhydrol.2018.08.050.

Zhang, B., Liu, C., Guo, Z., Liu, X., Liu, Y., 2018b. Probabilistic reservoir parameters inversion for anisotropic shale using a statistical rock physics model. Chin. J. Geophys.-Chin. Ed. 61 (6), 2601–2617. http://dx.doi.org/10.6038/cjg2018L0086.

Zhang, B., Liu, C., Guo, Z., Lu, N., Liu, X., 2017. Probabilistic reservoir-properties estimation for anisotropic shales using statistical rock physics and seismic data. In: SEG Technical Program Expanded Abstracts 2017. Society of Exploration Geophysicists, pp. 3179–3183. http://dx.doi.org/10.1190/segam2017-17784044.1.

Zhang, Y., Zhong, H.R., Wu, Z.Y., Zhou, H., Ma, Q.Y., 2020. Improvement of petrophysical workflow for shear wave velocity prediction based on machine learning methods for complex carbonate reservoirs. J. Pet. Sci. Eng. 192 (February), 107234. http://dx.doi.org/10.1016/j.petrol.2020.107234.